Over-Complete Source-Mapping Aided AMR-WB MIMO Transceiver Using Three-Stage Iterative Detection

N. S. Othman, M. El-Hajjar, A. Q. Pham, O. Alamri, S. X. Ng and L. Hanzo

School of ECS, University of Southampton, SO17 1BJ, UK.
Tel: +44-23-8059 3125, Fax: +44-23-8059 4508
Email: lh@ecs.soton.ac.uk, http://www-mobile.ecs.soton.ac.uk

Abstract – **In this paper we propose an iteratively detected Sphere Packing (SP) aided Differential Space-Time Spreading (DSTS) scheme using a Recursive Systematic Convolutional (RSC) code, for protecting the soft-bit assisted Adaptive Multi Rate Wideband (AMR-WB) decoder's bitstream, which is also protected by a novel over-complete source-mapping scheme. The convergence behaviour of the Multiple-Input Multiple-Output (MIMO) transceiver advocated is investigated with the aid of both three-dimensional (3D) and two-dimensional (2D) Extrinsic Information Transfer (EXIT) charts. The proposed system exhibits an E_b/N_0 gain of about 2.5 dB in comparison to the benchmark scheme carrying out iterative source- and channel-decoding as well as DSTS aided SP-demodulation, but dispensing with the over-complete source-mapping, when using $I_{system} = 3$ system iterations.**

1. MOTIVATION AND BACKGROUND

The employment of joint source and channel coding techniques has been motivated by the fact that the classic Shannonian source and channel coding separation theorem [1] has limited applicability in practical speech systems [2]. This is due to the delay- and complexity constraints of practical speech transmission systems. For example, iterative turbo decoding can be used to exploit the residual redundancy found in the encoded bitstream of finite-delay lossy speech codecs. This residual redundancy is inherently present owing to the limited-complexity, limited-delay source encoders' failure to remove all the redundancy from the correlated speech source signal.

Vary and his team [3, 4] developed the concept of soft speech bits exploiting the residual redundancy. Their work culminated in the formulation of iterative source and channel decoding (ISCD) [5]. More explicitly, in order to improve the overall system performance, *extrinsic* information is exchanged between the constituent decoders including the source decoder. As a further development, in [6] and [7] the inherent residual redundancy of the encoded bitstream was deliberately increased using redundant index assignments and multi-dimensional mapping schemes, which resulted in an enhanced soft-bit source decoder performance.

In [6], the iterative decoding behaviour of an ISCD scheme was studied using Extrinsic Information Transfer (EXIT) charts [8], for characterizing the achievable performance of the ISCD scheme exploiting the residual redundancy inherent in the source encoded bitstream. In this contribution we propose and investigate the jointly optimised ISCD scheme of Figure 1 invoking the Adaptive Multirate-Wideband (AMR-WB) speech codec [9] exploiting the intentionally increased residual redundancy of the AMR-WB encoded bitstream by using the novel over-complete source-mapping of [10], which is protected by a Recursive Systematic Convolutional (RSC) code. The resultant bitstream is transmitted using Differential Space-Time Spreading (DSTS) combined with Sphere Packing (SP) modulation [11] over a temporally correlated narrowband Rayleigh fading channel. More explicitly, in the resultant multi-stage scheme *extrinsic* information is exchanged amongst the three constituent decoders, namely the source decoder, the channel decoder and the DSTS-SP demapper. On the other hand, DSTS employing two transmit and a single receive antenna was invoked for the sake of providing spatial diversity gain with the aid of non-coherent detection, without the potentially high complexity of channel estimation. Moreover, this powerful wireless transceiver benefits from the employment of SP modulation introduced for the sake of increasing the coding gain of the DSTS scheme. Recently, in [12] the soft-bit assisted AMR-WB codec exploiting the concept of soft speech bits was employed in a multi-stage turbo detection process, which resulted in an enhanced Bit Error Ratio (BER) performance. By contrast, in this paper we study the achievable performance of the AMR-WB speech codec exploiting the intentionally increased residual redundancy of the AMR-WB encoded bitstream using over-complete source-mapping [10], while employing a three-dimensional (3D) EXIT-chart based procedure and its two-dimensional (2D) EXIT-chart projection technique [13, 14] for designing the optimum combination of receiver components. We will refer to this three-stage system as the DSTS-SP-RSC-AMRWB-OCM scheme.

The paper is structured as follows. In Section 2, the overall system model is described, while our EXIT chart analyis is provided in Section 3 with the aid of 3D EXIT charts and their 2D projections. Section 4 quantifies the performace of our proposed three-stage scheme, while our conclusions are offered in Section 5.

2. SYSTEM OVERVIEW

2.1. Transmitter

The DSTS-SP-RSC-AMRWB-OCM system model is depicted in Figure 1. As shown in Figure 1, *extrinsic* information is exchanged amongst all three constituent decoders, namely the source decoder, the RSC decoder and the SP-demapper. The AMR-WB speech codec is capable of supporting nine different bit rates [15], each of which may be activated in conjunction with different-rate channel codecs and different-throughput adaptive modem modes [16]. Similar near-instantaneously adaptive speech and video systems were designed in [2, 17]. In our prototype system investigated here the AMR-WB codec operates at 23.05 kbps, generating a set of 52 speech parameters encoded by a total of 461 bits per 20 ms frame for representing the 8 kHz bandwidth speech signal sampled at 16 kHz.

Each AMR-WB-encoded frame consists of a set of 52 parameters denoted by $\{\mathbf{v}_{1,\tau},\mathbf{v}_{2,\tau},\ldots,\mathbf{v}_{\kappa,\tau},\ldots,\mathbf{v}_{52,\tau}\}$, where $\mathbf{v}_{\kappa,\tau}$ represents an encoded parameter, $\kappa = 1, ..., K_\kappa$ denotes the index of each param-

The financial support of the Universiti Tenaga Nasional Malaysia, of Vodafone under the auspices of the Dorothy Hodgkin Postgraduate Award, of the Ministry of Higher Education of Saudi Arabia and that of the EPSRC, UK as well as that of the European Union in the framework of the Pheonix and Newcom projects is gratefully acknowledged.

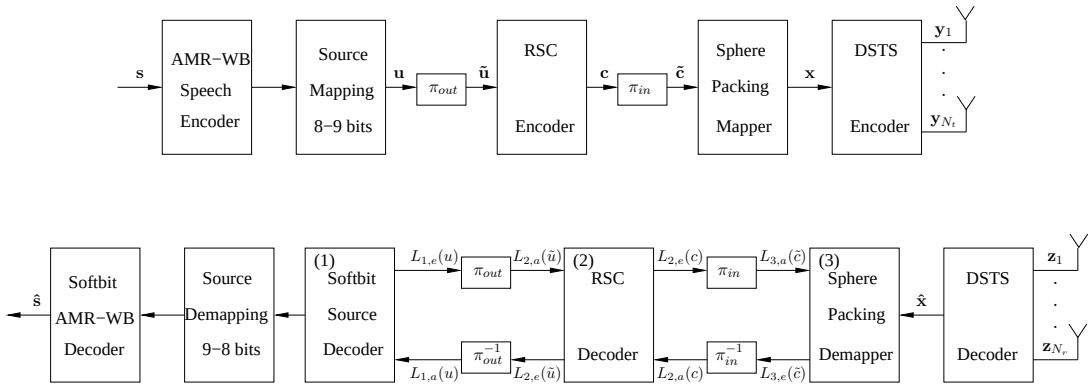

Figure 1: Block diagram of the DSTS-SP-RSC-AMRWB-OCM scheme. The notations $\mathbf{s}$, $\hat{\mathbf{s}}$, $\mathbf{u}$, $\mathbf{c}$, $\mathbf{x}$, $\mathbf{y}_j$, $\mathbf{z}_k$, π_{out} and π_{in} represent the frame of the speech source samples, the estimate of the speech source samples, the over-complete source-mapped bits of the encoded speech parameters, the encoded bits of the RSC encoder, the SP-coded symbols, the DSTS coded symbols of transmitter j, the received symbols at receiver k, the outer bit interleaver, and the inner bit interleaver, respectively. Furthermore, N_t and N_r denote the number of transmit and receive antennas, respectively.

eter in the encoded speech frame, $K_\kappa = 52$ and τ denotes the time index referring to the current encoded frame index.

However, in the advocated system we employ the over-complete source-mapping [10] using a rate of $R_{mapping}$=8/9. Thus, the AMR-WB encoded bitstream is divided into 8-bit source symbols $\tilde{\mathbf{v}}_{\kappa,\tau}$ = $[\tilde{v}(1)_{\kappa,\tau}\ \tilde{v}(2)_{\kappa,\tau}\ \ldots\ \tilde{v}(N)_{\kappa,\tau}]$, where $N = 8$ is the total number of bits assigned to the κth parameter. Then, $\tilde{\mathbf{v}}_{\kappa,\tau}$ is mapped to the bit sequence, $\mathbf{u}_{\kappa,\tau} = [u(1)_{\kappa,\tau}\ u(2)_{\kappa,\tau} \ldots u(M)_{\kappa,\tau}]$ using over-complete source-mapping, where $M = 9$. Then, the outer interleaver, π_{out} permutes the bits of the sequence $\mathbf{u}$, yielding $\tilde{\mathbf{u}}$ of Figure 1.

The bit sequence c of Figure 1 is the output of the RSC encoder, where a $\frac{3}{4}$-rate RSC code having a code memory of 3 and octally represented generator polynomials of $(G_1, G_2, G_3, G_4) = (11, 2, 4, 10)_8$ is employed. The RSC encoded bits are interleaved by interleaver π_{in} of Figure 1, which are then transmitted by using DSTS-SP. The SP-demapper maps B number of channel-coded bits $\tilde{\mathbf{c}}$=$[\tilde{c}_0\ \tilde{c}_1\ \ldots\ \tilde{c}_{B-1}] \in \{0,1\}$ to a SP symbol $x \in X$ as detailed in [11]. Furthermore, we have $B = \log_2(L_{SP}) = \log_2(16) = 4$, where L_{SP} represents the set of legitimate SP constellation points. Subsequently, we have a set of SP symbols that can be transmitted using DSTS and two transmit antennas, where one SP symbol is transmitted in two time slots, hence we have $R_{DSTS-SP}$=1/2, as detailed in [11]. In this study, we consider transmissions over a temporally correlated narrow-band Rayleigh fading channel, associated with a normalised Doppler frequency of $f_D = 0.01$.

Hence, the overall coding rate of the DSTS-SP-RSC-AMRWB-OCM scheme becomes R_{system} =464/708 ≈0.66. The effective spectral efficiency of the DSTS-SP-RSC-AMRWB-OCM scheme is $\log_2(L_{SP}) \cdot R_{system} \cdot R_{DSTS-SP}$ ≈1.31 bits per channel use.

2.2. Receiver

The notation $L(.)$ in Figure 1 denotes the LLRs of the bit probabilities. The notations $\tilde{c}$, c, $\tilde{u}$ and u in the round brackets $(.)$ of Figure 1 denote the SP bits, RSC coded bits, RSC data bits and the over-complete source-mapping aided AMR-WB encoded bits, respectively. The specific nature of the LLRs is represented by the subscripts of $L_{.,a}$, $L_{.,p}$ and $L_{.,e}$, denoting the *a priori*, *a posteriori* and *extrinsic* information, respectively, as shown in Figure 1. The LLRs associated with one of the three constituent decoders having a label of {1,2,3} are differentiated by the corresponding subscripts $(.)$ of {1,2,3}. Note that the subscript 2 is used for representing the RSC decoder of Figure 1.

Inner Iterations: The complex-valued received symbols $\mathbf{z}$ are demapped to their LLR [18] representation for each of the B number of RSC-encoded bits per DSTS-SP symbol. As seen in Figure 1, the *a priori* LLR values $L_{3,a}(\tilde{c})$ provided by the RSC decoder are subtracted from the *a posteriori* LLR values $L_{3,p}(\tilde{c})$ at the output of the SP-demapper for the sake of generating the *extrinsic* LLR values $L_{3,e}(\tilde{c})$. Then the LLRs $L_{3,e}(\tilde{c})$ are deinterleaved by a soft-bit deinterleaver. Next, the deinterleaved soft-bits $L_{2,a}(c)$ of Figure 1 are passed to the RSC decoder in order to compute the *a posteriori* LLR values $L_{2,p}(c)$ provided by the MAP algorithm [19] for all the RSC-encoded bits. The *extrinsic* information $L_{2,e}(c)$ seen in Figure 1 is generated by subtracting the *a priori* information $L_{2,a}(c)$ from the *a posteriori* information $L_{2,p}(c)$ according to $L_{2,e}(c) = L_{2,p}(c) - L_{2,a}(c)$, which is then fed back to the SP-demapper as the *a priori* information $L_{3,a}(\tilde{c})$ after appropriately reordering them using the inner soft-value interleaver. The SP-demapper of Figure 1 exploits the *a priori* information $L_{3,a}(\tilde{c})$ for the sake of providing improved *a posteriori* LLR values $L_{3,p}(\tilde{c})$ which are then passed to the RSC decoder and in turn, back to the SP-demapper for further iterations.

Outer Iterations: As seen in Figure 1, the *extrinsic* LLR values $L_{2,e}(\tilde{u})$ of the original uncoded systematic information bits are generated by subtracting the *a priori* LLR values $L_{2,a}(\tilde{u})$ of the RSC decoder from the LLR values $L_{2,p}(\tilde{u})$ of the original uncoded non-systematic information bits. Then, the LLRs $L_{2,e}(\tilde{u})$ are deinterleaved by the outer soft-bit deinterleaver. The resultant soft-bits $L_{1,a}(u)$ are passed to the SBSD [5] that computes the *extrinsic* LLR values $L_{1,e}(u)$, as detailed during our further discourse. These *extrinsic* LLR values are then fed back to the RSC decoder after appropriately reordering them in the specific order required by the RSC decoder for the sake of completing an outer iteration.

We define two inner iterations followed by one outer iteration as having one "system iteration" denoted as $I_{system} = 1$. The residual redundancy, which manifests itself in terms of the unequal probability of occurence of the M-ary source symbols is exploited as *a priori* information for computing the *extrinsic* LLR values.

The details of the algorithm used for computing the *extrinsic* LLR values $L_{1,e}(u)$ for the zero-order Markov model can be found in [5], which are briefly reviewed below. Firstly, the channel's output information related to each speech parameter is given by the product of each of the constituent bits as follows:

$$p(\hat{\mathbf{u}}_{\kappa,\tau}|\mathbf{u}_{\kappa,\tau}) = \prod_{m=1}^{M} p(\hat{u}_{\kappa,\tau}(m)|u_{\kappa,\tau}(m)), \tag{1}$$

where $\hat{\mathbf{u}}_{\kappa,\tau}$ =$[\hat{u}(1)_{\kappa,\tau}\ \hat{u}(2)_{\kappa,\tau}\ \ldots\ \hat{u}(M)_{\kappa,\tau}]$ is the received bit sequence of the κth parameter, while $\mathbf{u}_{\kappa,\tau}$ is the corresponding transmitted bit sequence provided that all these bits are independent of

each other. Hence, by excluding the bit under consideration from the present bit sequence within each of the κth parameter where $\kappa = 1, ..., K_\kappa$, namely from $\mathbf{u}_{\kappa,\tau}$=[$u_{\kappa,\tau}(m)$ $\mathbf{u}_{\kappa,\tau}^{[ext]}$], we obtain the *extrinsic* channel output information for each desired bit, $u_{\kappa,\tau}(\lambda)$:

$$p(\hat{\mathbf{u}}_{\kappa,\tau}^{[ext]}|\mathbf{u}_{\kappa,\tau}^{[ext]}) = \prod_{m\neq\lambda, m=1}^{M} p(\hat{u}_{\kappa,\tau}(m)|u_{\kappa,\tau}(m)), \quad (2)$$

where the term $\mathbf{u}_{\kappa,\tau}^{[ext]}$ denotes all elements of the bit pattern $\mathbf{u}_{\kappa,\tau}$, but excludes the desired bit $u_{\kappa,\tau}(\lambda)$ itself. Finally, the *extrinsic* LLR value $L_{1,e}(u)$ generated for each bit can be obtained by combining its channel output information and the *a priori knowledge* concerning the κth parameter, $p(\mathbf{u}_{\kappa,\tau})$, which is given by [5, 20]:

$$L_{S,e}(u_{\kappa,\tau}(\lambda)) = \log \frac{\sum_{\mathbf{u}_{\kappa,\tau}^{[ext]}} p(\mathbf{u}_{\kappa,\tau}^{[ext]}|u_{\kappa,\tau}(\lambda)=+1).p(\hat{\mathbf{u}}_{\kappa,\tau}^{[ext]}|\mathbf{u}_{\kappa,\tau}^{[ext]})}{\sum_{\mathbf{u}_{\kappa,\tau}^{[ext]}} p(\mathbf{u}_{\kappa,\tau}^{[ext]}|u_{\kappa,\tau}(\lambda)=-1).p(\hat{\mathbf{u}}_{\kappa,\tau}^{[ext]}|\mathbf{u}_{\kappa,\tau}^{[ext]})}, \quad (3)$$

where $p(\hat{\mathbf{u}}_{\kappa,\tau}^{[ext]}|\mathbf{u}_{\kappa,\tau}^{[ext]})$ can also be expressed in terms of the LLR values as [20]:

$$p(\hat{\mathbf{u}}_{\kappa,\tau}^{[ext]}|\mathbf{u}_{\kappa,\tau}^{[ext]}) = \Psi_{\kappa,\tau}^{[ext]} \exp\left[\sum_{u_{\kappa,\tau}(l) \text{ of } \mathbf{u}_{\kappa,\tau}^{[ext]}} \frac{u_{\kappa,\tau}(l)}{2}(L_{CD}^{[ext]}(u_{\kappa,\tau}(l)))\right] \quad (4)$$

and $L_{CD}^{[ext]}$ represents the *extrinsic* LLR values generated by soft-output channel decoding, while the product $\Psi_{\kappa,\tau}$ cancels out in Equation 3.

The proposed scheme's performance was studied against its benchmark scheme, which does not employ the over-complete source-mapping. We will refer to the benchmarker as the DSTS-SP-RSC-AMRWB scheme. The AMR-WB-encoded bitstream is protected by a $\frac{2}{3}$-rate RSC code having a code memory of 4 and octally represented generator polynomials of $(G_1, G_2, G_3) = (23, 2, 10)_8$. Thus, the overall coding rate of the DSTS-SP-RSC-AMRWB scheme dispensing with over-complete source-mapping becomes $R_{benchmark} = 464/708$ ≈0.66. The effective throughput of the DSTS-SP-RSC-AMRWB scheme dispensing over-complete source-mapping is $\log_2(L_{SP}) \cdot R_{benchmark} \cdot R_{DSTS-SP}$ ≈1.31 bit per channel use. In the benchmark scheme advocated, the soft-bit assisted AMR-WB speech decoder exploiting the natural residual redundancy, which manifests itself in terms of the unequal probability of occurence of the different values of a specific parameter in each 20 ms AMR-WB-encoded frame was invoked, as detailed in [12]. Thus, both the proposed DSTS-SP-RSC-AMRWB-OCM and the DSTS-SP-RSC-AMRWB benchmark schemes have the same overall coding rate and hence the same spectral efficiency.

3. EXIT-CHART ANALYSIS

EXIT charts have been widely used in the design of iterative schemes, since they facilitate the prediction of the associated convergence behaviour, based on the exchange of mutual information amongst the constituent receiver components.

As seen from Figure 1, the RSC decoder receives inputs from and provides outputs for both the SP-demapper and the SBSD. More explicitly, let $I_{.,A}(x)$ denote the mutual information (MI) [1] between the *a priori* value $A(x)$ and the symbol x, whilst $I_{.,E}(x)$ denotes the MI between the *extrinsic* value $E(x)$ and the symbol x. The MI associated with one of the three constituent decoders having a label of {1,2,3} is differentiated by the corresponding subscripts (.) of {1,2,3}. Thus, the input of the RSC decoder is constituted by the *a priori* input, $I_{2,A}(c)$ corresponding to the coded bits c originating from the *extrinsic* output of the SP-demapper as well as the *a priori* input, $I_{2,A}(\tilde{u})$, available for the data bits $\tilde{u}$, which was generated from the *extrinsic* output of the SBSD. Note that the subscript 2 is used for representing the RSC decoder of Figure 1.

Correspondingly, the RSC decoder generates both the *extrinsic* output, $I_{2,E}(c)$, representing the coded bits c as well as the *extrinsic* output, $I_{2,E}(\tilde{u})$ representing the data bits $\tilde{u}$. Therefore, the EXIT characteristic of the RSC decoder can be described by the following two EXIT functions [14]:

$$I_{2,E}(c) = T_c[I_{2,A}(\tilde{u}), I_{2,A}(c)], \quad (5)$$

$$I_{2,E}(\tilde{u}) = T_{\tilde{u}}[I_{2,A}(\tilde{u}), I_{2,A}(c)], \quad (6)$$

which are illustrated by the 3D surfaces seen in Figures 2 and 3, respectively.

By contrast, the SP decoder as well as the soft-bit source decoder only receive input from and provide output for the RSC decoder. Thus, the corresponding EXIT functions are:

$$I_{3,E}(\tilde{c}) = T_{\tilde{c}}[I_{3,A}(\tilde{c}), E_b/N_0], \quad (7)$$

for the SP decoder and

$$I_{1,E}(u) = T_u[I_{1,A}(u)], \quad (8)$$

for the SBSD. Equations (7) and (8) are illustrated in Figures 2 and 3, respectively.

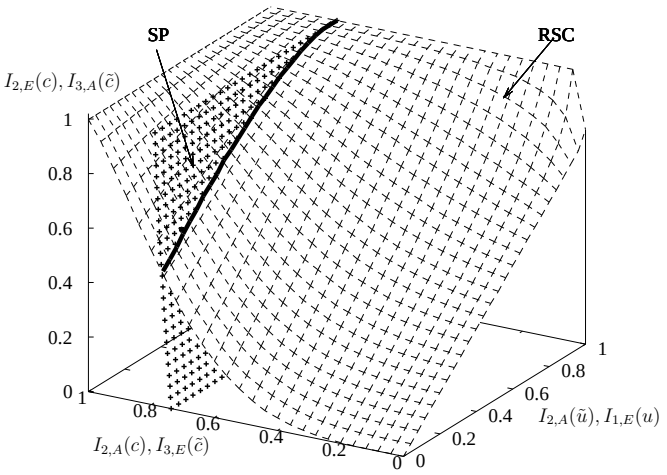

Figure 2: 3D EXIT chart of the RSC decoder and the SP-demapper at E_b/N_0=8.0 dB.

The EXIT chart analysis [8] of the iterative decoding scheme's convergence behaviour indicates that an infinitesimally low BER may only be achieved by an iterative receiver, if an open tunnel exists between the EXIT curves of the two Soft-In-Soft-Out (SISO) components.

More explicitly, the intersection of the surfaces seen in Figure 2 characterizes the best possible attainable performance, when exchanging information between the RSC decoder and the SP-demapper of Figure 1 for different fixed values of $I_{2,A}(\tilde{u})$, which is shown as a thick solid line. For each point $[I_{2,A}(\tilde{u}), I_{2,A}(c), I_{2,E}(c)]$ of this line on the 3D space of Figure 2, there is a specific value of $I_{2,E}(\tilde{u})$ determined by $I_{2,A}(\tilde{u})$ and $I_{2,A}(c)$ according to the EXIT function of Equation (6). Therefore the solid line on the surface of the EXIT function of the RSC decoder seen in Figure 2 is mapped to the solid line shown in Figure 3.

In order to avoid the somewhat cumbersome 3D representation, we project the bold EXIT curve of Figure 3 onto the 2D plane at

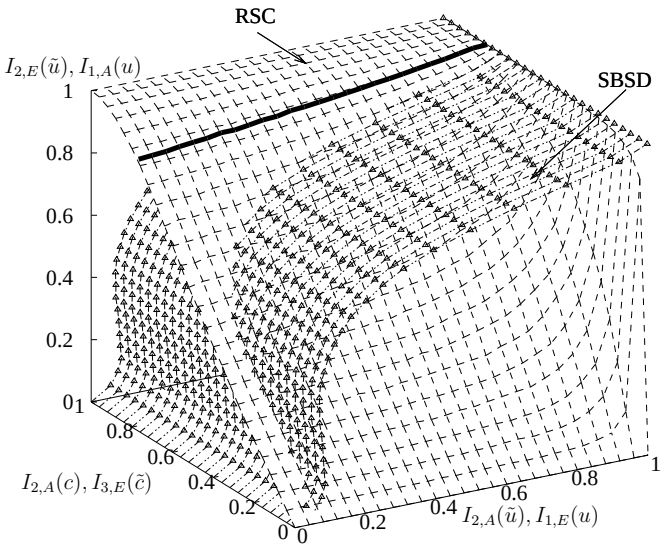

Figure 3: 3D EXIT chart of the RSC decoder and the soft-bit source decoder with projection from Figure 2.

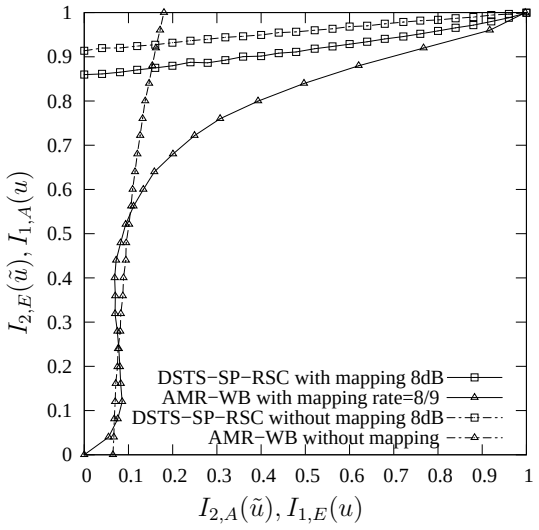

Figure 4: 2D projection of the EXIT chart of the proposed DSTS-SP-RSC-AMRWB-OCM scheme at E_b/N_0=8.0 dB.

$I_{2,A}(c) = 0$, yielding the line indicated by the squares in Figure 4. Also shown is the EXIT curve of the AMR-WB decoder employing over-complete source-mapping used in the advocated DSTS-SP-RSC-AMRWB-OCM scheme, which is denoted by the line marked with triangles.

We also carried out the EXIT chart analysis of the DSTS-SP-RSC-AMRWB benchmark scheme. More explicitly, the intersection of the RSC decoder and the SP-demapper's 3D surfaces results in a line, which characterizes the best possible attainable performance, when exchanging information between them. This line is then projected onto the 2D plane at an abscissa value of $I_{2,A}(c) = 0$ yielding the dotted line denoted with squares in Figure 4. However, in the DSTS-SP-RSC-AMRWB benchmark scheme a 2/3-rate RSC was invoked, as opposed to a 3/4-rate RSC employed in the DSTS-SP-RSC-AMRWB-OCM scheme. The soft-bit assisted AMR-WB decoder dispensing with the over-complete source-mapping is denoted by the dotted line marked with triangles in Figure 4.

As seen in Figure 4 the EXIT curve of the soft-bit assisted AMR-WB decoder cannot reach the convergence point of (1,1) and intersects with the EXIT curve of the projected curve, which implies that residual errors persist, regardless of both the number of iteration used and the size of the interleaver. On the other hand, by exploiting the intentionally imposed redundancy of the AMR-WB encoded bitstream using over-complete source-mapping resulted in reaching the point of convergence at (1,1). Thus, there is an open tunnel between the projected EXIT curve and that of the over-complete source-mapping assisted AMR-WB decoder at E_b/N_0=8.0 dB, as seen in Figure 4. Thus according to the EXIT chart predictions, the proposed system outperforms its benchmark scheme.

4. PERFORMANCE RESULTS

In this section, the attainable performance of the proposed scheme is characterised in terms of BER and Segmental Signal to Noise Ratio (SegSNR) [2] evaluated at the speech decoder's output as a function of the channel Signal to Noise Ratio (SNR) per bit.

We consider a two-transmit-antenna aided DSTS-SP system associated with $L_{SP} = 16$ and a single receive antenna. The remaining simulation parameters were described in Section 2. In our simulations, a single three-stage "system iteration" is constituted by two inner iterations followed by an outer iteration.

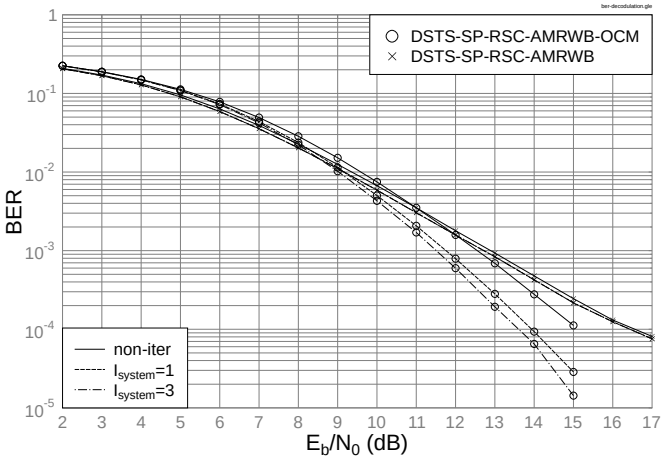

Figure 5: BER versus E_b/N_0 performance of the jointly optimised DSTS-SP-RSC-AMRWB-OCM scheme of Figure 1, when communicating over temporally correlated narrowband Rayleigh fading channels.

Figure 5 depicts the BER versus SNR per bit, namely versus E_b/N_0 performance of the DSTS-SP-RSC-AMRWB-OCM scheme and that of its corresponding DSTS-SP-RSC-AMRWB benchmark scheme. It can be seen from Figure 5 that the DSTS-SP-RSC-AMRWB-OCM scheme outperforms the DSTS-SP-RSC-AMRWB benchmark scheme by about 2.5 dB at BER=1×10^{-4} after $I_{system} = 3$ iterations, where again we define a "system iteration" I_{system} as having two inner iterations followed by a single outer-iteration, as mentioned in Section 2. The AMR-WB-decoded scheme employing over-complete source-mapping has a lower BER at its speech-decoded output than its benchmarker dispensing with over-complete source-mapping, because the intentionally added residual redundancy of the AMR-WB-encoded bitstream has imposed the EXIT-characteristics of the soft-bit source decoder, which resulted in an enhanced attainable BER.

In Figure 6 we plot the speech SegSNR performance of the proposed scheme and the benchmark scheme versus E_b/N_0. It can be seen from Figure 6 that the exploitation of the deliberately increased

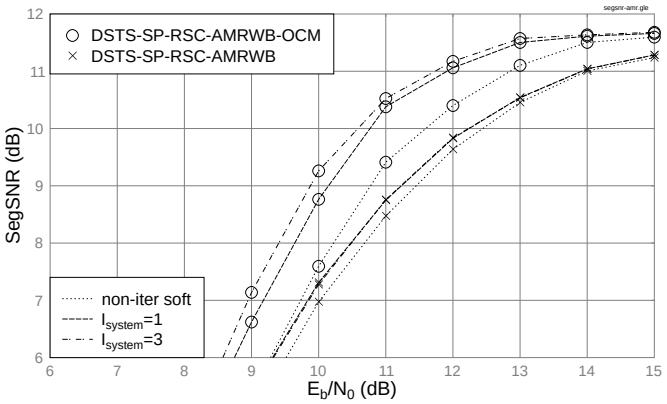

Figure 6: Average SegSNR versus E_b/N_0 performance of the jointly optimised DSTS-SP-RSC-AMRWB-OCM scheme of Figure 1 in comparison to the DSTS-SP-RSC-AMRWB benchmark scheme, when communicating over temporally correlated narrowband Rayleigh fading channels.

residual redundancy in the AMR-WB encoded bitstream has resulted in a E_b/N_0 gain of about 2 dB after $I_{system} = 3$ iterations, when tolerating a SegSNR degradation of 1 dB.

More explicitly, the DSTS-SP-RSC-AMRWB scheme has no OCM scheme, only a rate $R_2 = \frac{2}{3}$ channel encoder, while the DSTS-SP-RSC-AMRWB-OCM scheme employs a rate $R_1 = \frac{8}{9}$ OCM scheme combined with a rate $R_2 = \frac{3}{4}$ channel encoder. Although both schemes have the same overall coding rate of $R_{system} = R_{benchmark} = 2/3$, the latter assigns part of its channel encoder's redundancy to the OCM scheme and this is in addition to the source residual redundancy inherited in the source-encoded bitstream. It was shown in Section 3 that the assignment of channel encoder's redundancy to the OCM created an open EXIT chart tunnel right through to the convergence point of (1,1) even at a low SNR. The DSTS-SP-RSC-AMRWB-OCM scheme, which benefits from "an early" convergence outperforms the benchmark scheme having the same effective spectral efficiency.

In this contribution, we showed that the joint design of source and channel coding was beneficial where the redundancy allocation was appropriately apportioned for the OCM and channel encoders. The achievable performance was contrasted to that of the benchmark scheme where the redundancy was assigned entirely to the channel encoder. Our results also demonstrated that both iterative detection and the appropriate redundancy allocation between the OCM and channel codecs is crucial in the design of powerful joint source and channel coding schemes.

5. CONCLUSIONS

In this contribution the three-stage DSTS-SP-RSC-AMRWB-OCM scheme of Figure 1 was proposed for transmission over a temporally correlated narrowband Rayleigh fading channel. The employment of the over-complete source-mapping scheme, which delibrately imposed redundancy on the AMR-WB-encoded bitstream provided a significant improvement in terms of the average SegSNR versus channel E_b/N_0 performance compared to its corresponding benchmark scheme dispensing with over-complete source-mapping. The performance of the proposed transceiver is about 2.5 dB better in terms of the E_b/N_0 in comparison to the three-stage benchmark scheme, but dispensing with over-complete source-mapping.

6. REFERENCES

[1] C. E. Shannon, "A Mathematical Theory of Communication," *The Bell System Technical Journal*, vol. 27, pp. 379–423,623–656, July, October 1948.

[2] L. Hanzo, F.C.A. Somerville and J.P. Woodard, *Voice and Audio Compression for Wireless Communications, 2nd Edition*. Chichester, UK: John Wiley-Sons Inc., 2007.

[3] T. Fingscheidt and P. Vary, "Speech Decoding with Error Concealment using Residual Source Redundancy," *IEEE Workshop on Speech Coding for Telecommunication*, pp. 91–92, 7-10 Sept 1997.

[4] T. Fingscheidt and P. Vary, "Softbit Speech Decoding: A New Approach to Error Concealment," *IEEE Transactions on Speech and Audio Processing*, vol. 9, pp. 240–251, March 2001.

[5] M. Adrat, P. Vary and J. Spittka, "Iterative Source-Channel Decoder Using Extrinsic Information from Softbit-Source Decoding," *IEEE International Conference on Acoustics, Speech and Signal Processing*, pp. 2653–2656, 7-11 May 2001.

[6] M. Adrat and P. Vary, "Iterative Source-Channel Decoding: Improved System Design Using EXIT Charts," *EURASIP Journal on Applied Signal Processing*, pp. 1727–1737, October 2005.

[7] T. Clevorn, M. Adrat and P. Vary, "Turbo Decodulation Using Highly Redundant Index Assignments and Multi-Dimensional Mappings," *4th Int. Symposium on Turbo Codes and Related Topics in connection with 6th Int. ITG-Conference on Source and Channel Coding*, April 2006.

[8] S. ten Brink, "Convergence Behaviour of Iteratively Decoded Parallel Concatenated Codes," *IEEE Transactions on Communications*, vol. 49, pp. 1727–1737, October 2001.

[9] B. Bessette, R. Salami, R. Lefebvre, M. Jelinek, J. Rotola-Pukkila, J. Vainio, H. Mikkola and K. Jarvinen, "The Adaptive Multirate Wideband Speech Codec (AMR-WB)," *IEEE Transactions on Speech and Audio Processing*, vol. 10, pp. 620–636, November 2002.

[10] A. Q. Pham, L. Hanzo and L. L-. Yang, "Joint Optimization of Iterative Source and Channel Decoding Using Over-Complete Source-Mapping," in *IEEE 66th Vehicular Technology Conference*, 30 Sept.-3 Oct 2007, http://eprints.ecs.soton.ac.uk/14461/.

[11] M. El-Hajjar, O. Alamri and L. Hanzo, "Differential Space-Time Spreading Using Iteratively Detected Sphere Packing Modulation and Two Transmit Antennas," in *IEEE Wireless Communications and Networking Conference*, vol. 3, pp. 1664–1668, April 2006.

[12] N. S. Othman, M. El-Hajjar, O. Alamri and L. Hanzo, "Soft-Bit Assisted Iterative AMR-WB Source-Decoding and Turbo-Detection of Channel-Coded Differential Space-Time Spreading Using Sphere Packing Modulation," *IEEE 65th Vehicular Technology Conference*, pp. 2010–2014, 22-25 April 2007.

[13] M. Tüchler, "Convergence Prediction for Iterative Decoding of Threefold Concatenated Systems," *IEEE Global Telecommunications Conference*, vol. 2, pp. 1358–1362, 17-21 November 2002.

[14] F. Brännström, L. K. Rasmussen and A. J. Grant, "Convergence Analysis and Optimal Scheduling for Multiple Concatenated Codes," *IEEE Transactions on Information Theory*, vol. 51, pp. 3354–3364, September 2005.

[15] 3GPP TS 26.190 V5, "AMR Wideband Speech Codec: Transcoding Functions," December 2001.

[16] L. Hanzo, C. H. Wong and M. S. Yee, *Adaptive Wireless Transceivers: Turbo-Coded, Turbo-Equalized and Space-Time Coded TDMA, CDMA, and OFDM Systems*. New York, USA : John Wiley and Sons, 2002.

[17] L. Hanzo, P.J. Cherriman and J. Streit, *Video Compression and Communications: H.261, H.263, H.264, MPEG4 and Proprietary Codecs*. New York: John Wiley-Sons Inc., 2007.

[18] L. Hanzo, T. H. Liew and B. L. Yeap, *Turbo Coding, Turbo Equalisation and Space Time Coding for Transmission over Wireless channels*. New York, USA: John Wiley IEEE Press, 2002.

[19] P. Robertson, E. Villebrun and P. Hoeher, "A Comparison of Optimal and Sub-Optimal MAP Decoding Algorithms Operating in the Log Domain," *IEEE International Conference on Communications*, vol. 2, pp. 1009–1013, 18-22 June 1995.

[20] M. Adrat, *Iterative Source-Channel Decoding for Digital Mobile Communications*. RWTH Aachen University: Ph.D Dissertation, 2003.